Dynamic shape space modeling with change points

Peihua Qiu, University of Florida
Anuj Srivastava, Florida State University
Chiwoo Park, University of Washington

2024 AFOSR Dynamical Systems and Control Theory Program Review

This project is partially supported by FA9550-23-1-0673

Interested in modeling dynamical systems with shape states

- Time index, $t \in \mathcal{T}$
- System state, $X_t \in \mathcal{X}$: geometrical shape of an d-dimensional object (exterior outline, skeleton, ...)
- Control input, $u_t \in \mathbb{R}^p$: p real control inputs.
- Uncontrollable external factors ϵ_t,

Shape evolution with regime changes

- The state evolution occurs in a piecewise manner with K regimes,

$$X_{t+1} = f_k(t, X_t, u_t, \epsilon_t) \text{ for the } k\text{th regime}, k = 1, ..., K. \tag{1}$$

- Regime changes: Regimes change in the domain

$$\Omega = \mathcal{T} \times \mathcal{X} \times \mathbb{R}^p.$$

  One can consider a partition of the domain,

$$\Omega = \bigcup_{k=1}^{K} \Omega_k,$$

  with Ω_k representing the kth regime.

- Change points: The boundaries delineating the regimes are referred to as change points. They are assumed smooth.

Objective

- Our major interest is the data-driven representation of the state evolution. It can be potentially useful for data-driven control of the state evolution.
- Representation of the shape space and piece-wise state space,

$$X_{t+1} = f_k(t, X_t, u_t, \epsilon_t)$$

- Estimation of the change points (or Ω_k) jointly with the component model in the shape space.

Primary Testbed: Additive Manufacturing

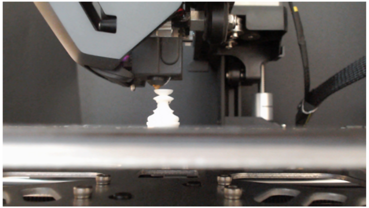

Control inputs:
Temperature: 100 to 300
Feed rate: 0 to 200
Flow rate: 0 to 200

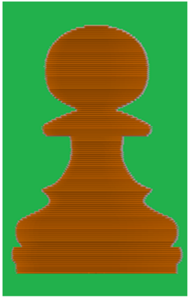

(a) CAD model image

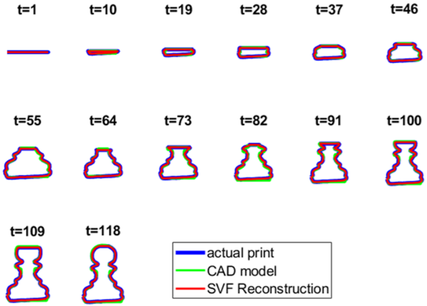

(b) Shapes of Actual Prints

- Collaborator: Benji Maruyama, Autonomous Materials Lead, Materials & Manufacturing Directorate at Air Force Research Laboratory
- Benchmark data and metrics

Other Testbeds

(a) Evolutions

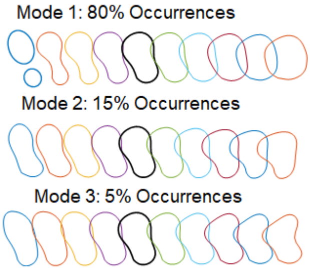

nanoparticle morphology evolutions under different conditions

(with Woehl at U. Maryland)

(b) Interactions

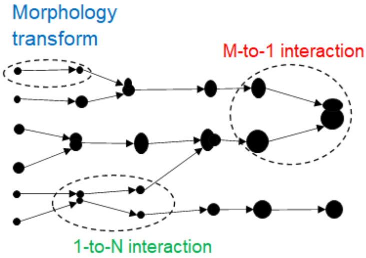

nanoparticle interactions during their self-assemblies

(with Browning at U. of Liverpool)

(c) Motions

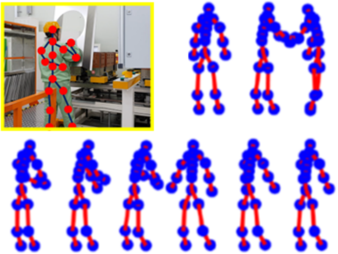

Worker motions in a manufacturing factory for operations research

(with Noh at Sungkyunkwan Univ.)

Major Challenges..

Mathematical representations of shapes are not straightforward.

- Shape is defined as a property that is invariant to certain transformations such as rotation, translation and scale.

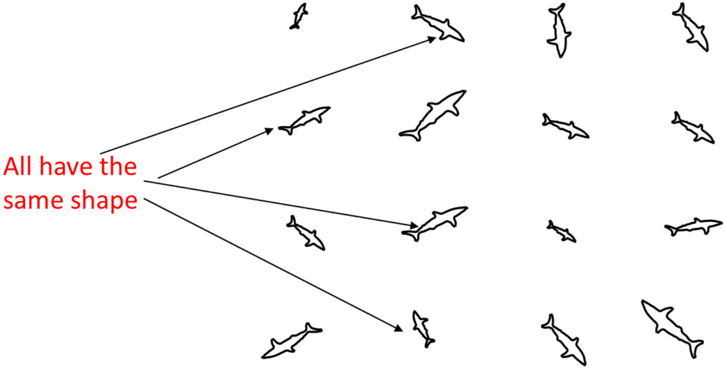

Shape Spaces are Non-Euclidean.

- Due to the need for invariance, the shape space is non-Euclidean. Shape spaces are nonlinear spaces, not vector spaces.
- We cannot simply add, subtract shapes, or average shapes.
- Shape analysis requires tools from differential geometry to handle nonlinear nature of shape representations.

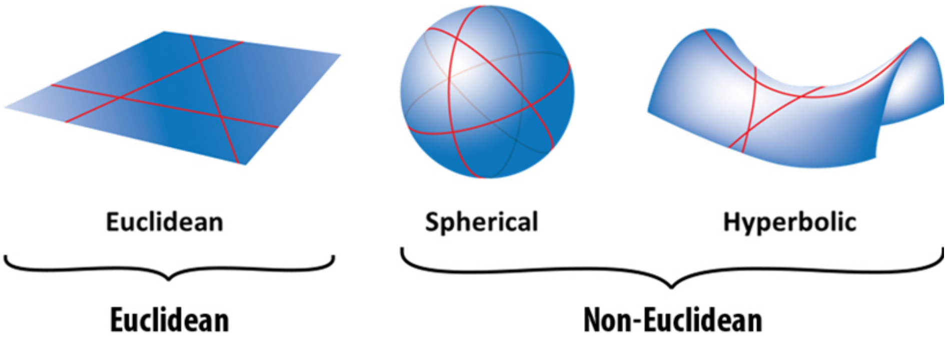

Shape space: Landmark-based approach...

Landmark Data

$$\boldsymbol{X} = [x_1, x_2, \ldots, x_n]$$

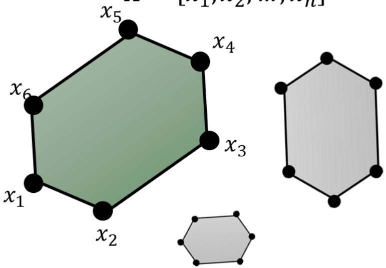

Pre-shape

Centering:

$$\boldsymbol{X_c} = [\hat{x}_1, \hat{x}_2, \ldots, \hat{x}_n]$$

$$\hat{x}_k = x_k - \frac{1}{n}\sum_{j=1}^{n} x_j$$

Scaling:

$$\boldsymbol{X_p} = \frac{\boldsymbol{X_c}}{||\boldsymbol{X_c}||}$$

A pre-shape $\boldsymbol{X_p}$ is a point in a hypersphere in R^{2n}.

Shape

A shape of $\boldsymbol{X_p}$ is an equivalent class of pre-shapes under rotation operator $\boldsymbol{O}$.

$$[\boldsymbol{X_p}] = \{\boldsymbol{O}\boldsymbol{X_p}, \boldsymbol{O} \in \mathrm{SO(n)}\}$$

A shape $[\boldsymbol{X_p}]$ is an orbit of a hypersphere in R^{2n}.

Reference: Kendall et al. (2009)

Shape space: Contour-based approach...

Parametric curve outlining an object

$X_t: S^{d-1} \to R^d$

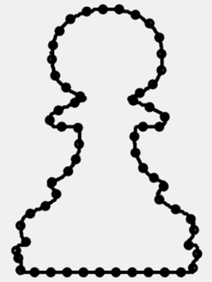

Pre-shape

Pre-shape is invariant to the location and scale transformation of an object.

$$X_t \mapsto q_t = \frac{dX_t}{\sqrt{||dX_t||}}$$

Shape

Shape is an equivalent class of pre-shapes under rotation operator O and reparameterization γ

$$[q_t] = \{O\,(q_t \circ \gamma): O \in SO(d), \gamma: S^{d-1} \to S^{d-1}\}$$

$[q_t]$ is an orbit of an infinite-dimensional hypersphere.

Reference: Srivastava and Klassen (2016)

Major challenges...

- The shape space $\mathcal{X}$ is infinite-dimensional and non-Euclidean. Modeling the state evolution over time in an infinite-dimensional non-Euclidean space is challenging: Addressed by the U. of Washington and Florida State U. Team.
- Change point detection in a high dimensional space is an extremely challenging problem: Addressed by the U. of Florida Team.

Main Outcome 1. State Evolution Modeling with States in Riemannian Manifold

Our Goal: Modeling Dynamic Shapes

- Develop statistical models for capturing shapes evolving over time.
- We model them as stochastic processes over time.

Two Approaches:

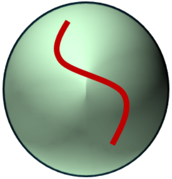

1. Intrinsic Approach. (Difficult and Accurate): Model the process on the manifold directly and intrinsically.

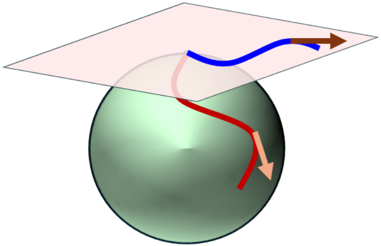

2. Flattening Approach. (Simpler and Approximate): Map the process to a Euclidean (tangent) space and then apply traditional models.

Multiple flattening ideas...

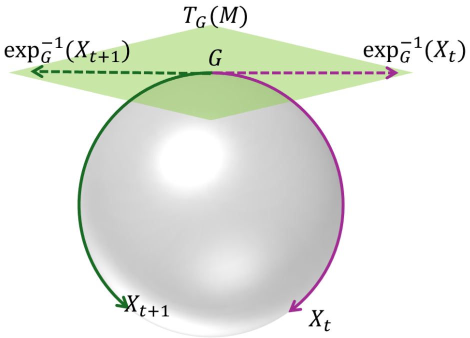

- Here one selects a reference point G on manifold M and maps all other point from manifold to the tangent space $T_G(M)$ using inverse exponential map.
- Simple but the distortion in distances between points far from G is large.

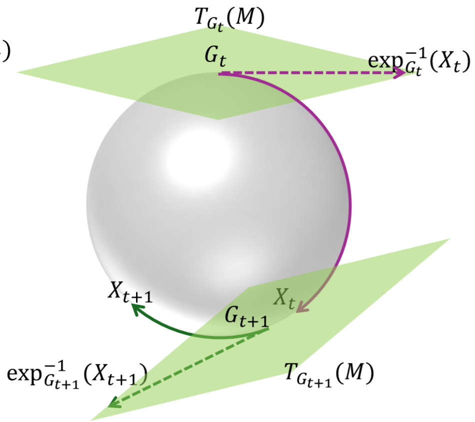

- Approximating with multiple tangent spaces results in multiple vector spaces.

Reference for idea (a): Yi et al. (2012)

Transporting multiple tangent spaces to one reference tangent space...

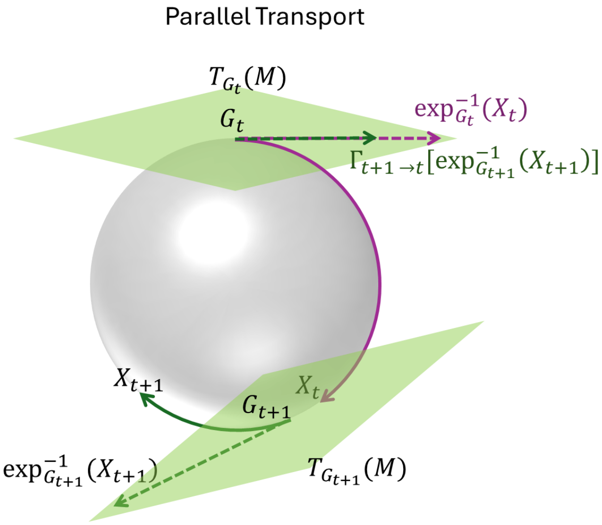

- Take the parallel transport of all tangent vectors to one reference tangent space along geodesic.
- So, all tangent vectors belong to one vector space. We can do PCA for dimensional reductions and use vector autoregressive models to model their transitions.

Details...

Let $\mathcal{M}$ denote infinite dimensional shape manifold, i.e. space of $[q_t]$'s. For each t,

- Take the local reference shape $G_t \in \mathcal{M}$.
- Take the tangent vector of X_t around G_t,

$$\boldsymbol{\omega}_t = \exp_{G_t}^{-1}(X_t) \in \mathcal{T}_{G_t}(\mathcal{M}).$$

- Perform the parallel transport $\boldsymbol{\omega}_t$ along the geodesic from $\mathcal{T}_{G_t}(\mathcal{M})$ and $\mathcal{T}_{G_T}(\mathcal{M})$,

$$\boldsymbol{v}_t = \Gamma_{t \to T}[\exp_{G_t}^{-1}(X_t)] \in \mathcal{T}_{G_T}(\mathcal{M}).$$

We name this representation of a shape sequence as the single-hop transported vector field (SH-TVF).

Special Case: Velocity-Preserving Vector Field

- When one takes the local reference shape $G_t = X_{t-1}$,
$$\boldsymbol{v}_t = \Gamma_{t \to T}[\exp^{-1}_{G_t}(X_t)] \in \mathcal{T}_{G_T}(\mathcal{M})$$
represents the local velocity of X_t.
- Integrating the velocity, we can create the vector representation of the original shape sequence X_t,
$$\boldsymbol{\mu}_t = \sum_{i=1}^{T} \boldsymbol{v}_i.$$
- Property. Euclidean distance between $\boldsymbol{\mu}_{t-1}$ and $\boldsymbol{\mu}_t$ = Geodesic distance between of $\boldsymbol{X}_{t-1}$ and $\boldsymbol{X}_t$.
- Property. Derivative of the vector field $\boldsymbol{\mu}_t$= Derivative of the original shape sequence X_t.
- One can completely construct the original shape sequence with the vector field.

Our Approach: Space Evolution

- Start with the simplest possible.
- Perform PCA on $\{\boldsymbol{v}_t\}$,

$$\boldsymbol{z}_t = \boldsymbol{P}\boldsymbol{v}_t.$$

- Fit a simple AR(1) model,

$$\boldsymbol{z}_{t+1} = \boldsymbol{A}_k \boldsymbol{z}_t + \boldsymbol{B}_k \boldsymbol{u}_t + \boldsymbol{\epsilon}_t, \tag{2}$$

  where $(\boldsymbol{A}_k, \boldsymbol{B}_k)$ is specific to control regime $k = 1, ..., K$.
- For the time being, we forget about regime changes and test the idea with single regime.

Numerical Example: 3D Print

- Printing a chess pawn sliced into 118 vertical layers

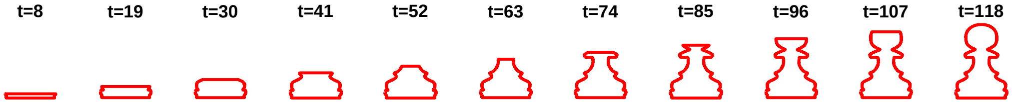

- After each layer is printed, the shape of the print result is recorded, which is X_t, $t = 1, 2, ..., 118$.
- Three control inputs ($\boldsymbol{u}_t$): feed rate, flow rate, temperature
- Run 16 printing experiments and takes 16 shape sequences. Randomly split the 16 sequences into 70% training and 30% test datasets.
- With the training data, we learned the SH-TVF representations z_t (the PCA dimension 35 reserves 80% of the total variations).

Representation Error = Shape geodesic distance between the actual print and the reconstructed shape

Total Variation Reserved	50%	60%	70%	80%	90%	100%
PCA Dimension p	10	15	22	35	62	400
Error (in Shape Distance)	0.3338	0.2994	0.2629	0.2139	0.1544	0.0178*

Table: PCA Reconstruction Error. * The error for the 100% case should be theorectically zero. The non-zero error number for the column with the 100% case could be regarded as a small numerical error.

SH-TVF Representation with $p = 35$

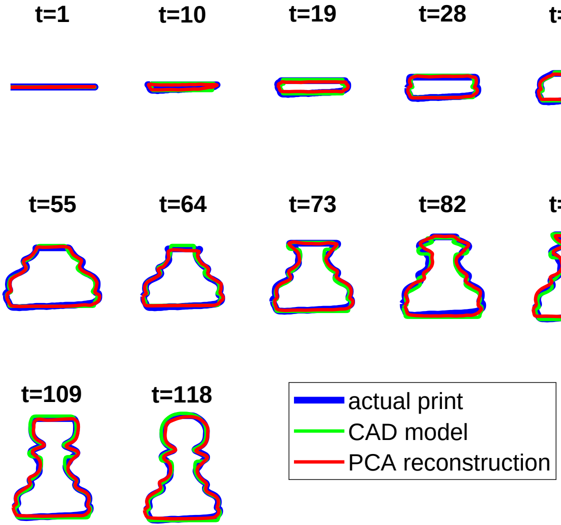

Predictability.

- With the training data, we fit a simple linear state space equation,

$$\boldsymbol{z}_{t+1} = \boldsymbol{A}\boldsymbol{z}_t + \boldsymbol{B}\boldsymbol{u}_t + \boldsymbol{\epsilon}_t. \tag{3}$$

  with single control regime.
- Applied the fitted model to predict shape sequences. The prediction error is measured

Forecasting Step	1	2	3	4
Training Error	0.2418	0.2722	0.2965	0.3142
Test Error (Training: 14 seq, Test: 6 seq)	0.2581	0.3050	0.3371	0.3581

Table: Model Prediction Error versus PCA Error 0.2139. All errors are measured by the shape geodesic distance.

Poor predictability for some sub regions suggests control regime changes.

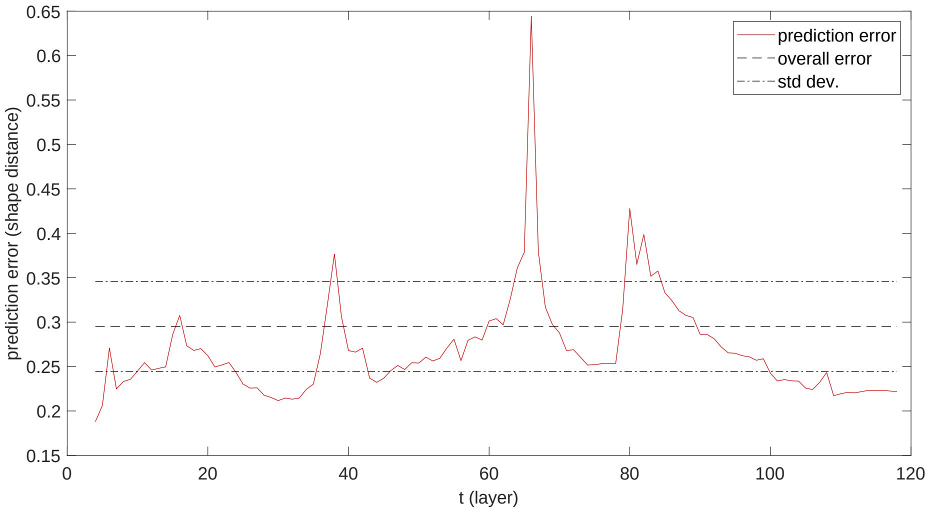

Main Outcome 2. Change Point Detection in Shape State Space Model

Goal: Detecting change points to delineate control regimes

- **Offline change-point detection problem**: To estimate control regimes $\{\Omega_k, k = 1, ..., K\}$ and the model parameters $\{\boldsymbol{A}_k, \boldsymbol{B}_k, k = 1, ..., K\}$.

$$\boldsymbol{z}_{t+1} = \boldsymbol{A}_k \boldsymbol{z}_t + \boldsymbol{B}_k \boldsymbol{u}_t + \boldsymbol{\epsilon}_t, (t, \boldsymbol{z}_t, \boldsymbol{u}_t) \in \Omega_k. \tag{4}$$

- Many change point detection methods are focused on detecting the changes in the state $\boldsymbol{z}_t$, instead of the model parameters $\boldsymbol{A}_k$ and $\boldsymbol{B}_k$ (Hawkins, 2001).
- Detecting changes in $\boldsymbol{A}_k$ and $\boldsymbol{B}_k$ has been studied for univariate time series (Box and Tiao, 1965; Gombay, 2008) but not for multivarite time series.

First study the simplest setup..

- $K = 2$ with a single change-point $t = r$:

$$\begin{cases} \mathbf{z}_{t+1} = \mathbf{A}_1 \mathbf{z}_t + \mathbf{B}_1 \mathbf{u}_t + \boldsymbol{\epsilon}_t & 1 \le t \le r-1, \\ \mathbf{z}_{t+1} = \mathbf{A}_2 \mathbf{z}_t + \mathbf{B}_2 \mathbf{u}_t + \boldsymbol{\epsilon}_t & r \le t \le T-1. \end{cases}$$

  The error terms $\boldsymbol{\epsilon}_t$ are i.i.d. from $\mathrm{N}_p(\mathbf{0}, \sigma^2 \mathbf{I}_p)$

- We aim to obtain estimates of the change-point location r, transition matrices before and after the change point and the variance of the error terms.

Maximum Likelihood Estimation

- Consider N training sequences with the ith sequence represented by

$$(\boldsymbol{z}_{i,t}, \boldsymbol{u}_{i,t}), i = 1, ..., N, t = 1, ..., T. \tag{5}$$

- We aim to obtain MLEs for $\boldsymbol{\theta} = \{r, \mathbf{A}_1, \mathbf{B}_1, \mathbf{A}_2, \mathbf{B}_2, \sigma^2\}$.
- The log-likelihood of the change-point problem can be expressed as

$$l(\boldsymbol{\theta}) = -\frac{NTp}{2}\log\sigma^2 - \frac{1}{2\sigma^2}\sum_{i=1}^{N}\sum_{t=0}^{r-1}||\mathbf{z}_{i,t+1} - \mathbf{A}_1\mathbf{z}_{it} - \mathbf{B}_1\mathbf{u}_{it}||_2^2$$
$$-\frac{1}{2\sigma^2}\sum_{i=1}^{N}\sum_{t=r}^{T-1}||\mathbf{z}_{i,t+1} - \mathbf{A}_2\mathbf{z}_{it} - \mathbf{B}_2\mathbf{u}_{it}||_2^2.$$

where $||\cdot||_2^2$ is the l^2-norm operator.

Maximum Likelihood Estimation

- Conditioned on r, the MLE of $\mathbf{A}_1, \mathbf{B}_1, \mathbf{A}_2, \mathbf{B}_2$ can be expressed in the closed form, e.g.,

$$\begin{pmatrix} \text{vec}(\widetilde{\mathbf{A}}_1(r)) \\ \text{vec}(\widetilde{\mathbf{B}}_1(r)) \end{pmatrix} = \begin{pmatrix} \left(\sum_{i=1}^N \sum_{t=0}^{r-1} \mathbf{z}_{it}\mathbf{z}_{it}^T\right)^T \otimes \mathbf{I}_d & \left(\sum_{i=1}^N \sum_{t=0}^{r-1} \mathbf{u}_{it}\mathbf{z}_{it}^T\right)^T \otimes \mathbf{I}_d \\ \left(\sum_{i=1}^N \sum_{t=0}^{r-1} \mathbf{z}_{it}\mathbf{u}_{it}^T\right)^T \otimes \mathbf{I}_d & \left(\sum_{i=1}^N \sum_{t=0}^{r-1} \mathbf{u}_{it}\mathbf{u}_{t}^T\right)^T \otimes \mathbf{I}_d \end{pmatrix}^{-} \begin{pmatrix} \text{vec}\left(\sum_{i=1}^N \sum_{t=0}^{r-1} \mathbf{z}_{i,t+1}\mathbf{z}_{it}^T\right) \\ \text{vec}\left(\sum_{i=1}^N \sum_{t=0}^{r-1} \mathbf{z}_{i,t+1}\mathbf{u}_{it}^T\right) \end{pmatrix},$$

- $\widehat{r} = \text{argmin}_{1 \le r \le (T-1)} \Big\{ \sum_{i=1}^N \sum_{t=0}^{r-1} ||\mathbf{z}_{i,t+1} - \widetilde{\mathbf{A}}_1(r)\mathbf{z}_{it} - \widetilde{\mathbf{B}}_1(r)\mathbf{u}_{it}||_2^2 +$
  $\sum_{i=1}^N \sum_{t=r}^{T-1} ||\mathbf{z}_{i,t+1} - \widetilde{\mathbf{A}}_2(r)\mathbf{z}_{it} - \widetilde{\mathbf{B}}_2(r)\mathbf{u}_{it}||_2^2 \Big\}.$
- After obtaining the change-point location $\widehat{r}$, MLE of other parameters can be computed accordingly.

Numerical Results

- Apply the proposed method to the 3d-print case, resulting in $\widehat{r} = 65$.

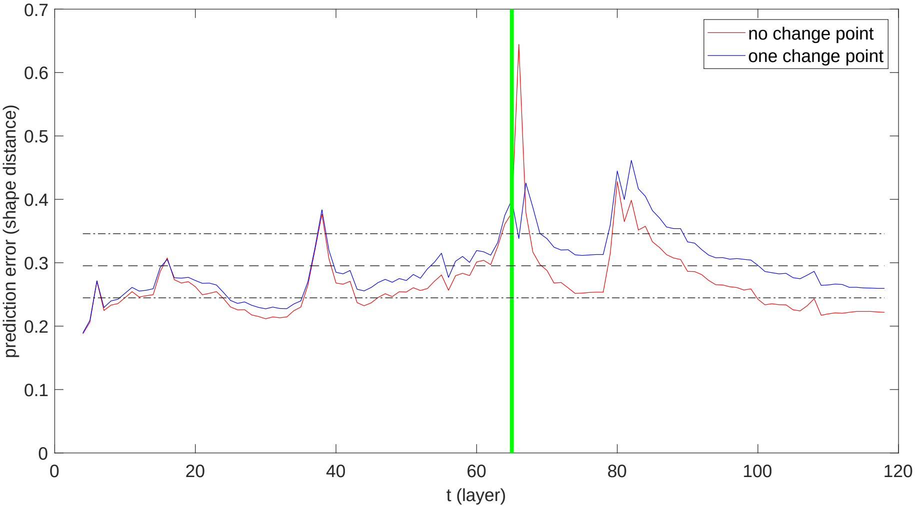

Summary...

- Shape sequence. Developed the SH-TVF representation of a shape sequence and studied a piece-wise linear state space model over it.
- Regime changes. Started to work on the offline change point detection problem with the simplest setup.
- Supported Graduate Students: Yanliang Chen (Florida State University), Zibo Tian (U. of Florida)
- On-going Publications:
  Chen et al. (2024) Statistical Emulators for Human Shape Sequences. To be submitted soon to the journal *Operations Research*.

Plan for the Next Year

- SH-TVF: Single-hop parallel transport versus multi-hop parallel transport
- State Space: Linear state space versus locally linear state space.
- Change points: single change point versus multiple changed-points (number of change-points need to be estimated).
- Change points along one covariate versus multivariate change points.
- Offline change points versus online change points
- Study theoretical properties of the estimator(s) for the change-point location(s).

References I

Box, G. E. and Tiao, G. C. (1965). A change in level of a non-stationary time series. *Biometrika*, 52(1/2):181–192.

Chen, Y., Park, C., and Srivastava, A. (2024). Statistical emulators for human shape sequences. *Operations Research*, pages 1–30.

Gombay, E. (2008). Change detection in autoregressive time series. *Journal of Multivariate Analysis*, 99(3):451–464.

Hawkins, D. M. (2001). Fitting multiple change-point models to data. *Computational Statistics & Data Analysis*, 37(3):323–341.

Kendall, D. G., Barden, D., Carne, T. K., and Le, H. (2009). *Shape and shape theory*. John Wiley & Sons.

Srivastava, A. and Klassen, E. P. (2016). *Functional and shape data analysis*, volume 1. Springer.

Yi, S., Krim, H., and Norris, L. K. (2012). Human activity modeling as brownian motion on shape manifold. In Bruckstein, A. M., ter Haar Romeny, B. M., Bronstein, A. M., and Bronstein, M. M., editors, *Scale Space and Variational Methods in Computer Vision*, pages 628–639, Berlin, Heidelberg. Springer Berlin Heidelberg.